

AD \_\_\_\_\_

Award Number: W81XWH-10-1-0196

TITLE: Exosomal microRNA Signatures in the Diagnosis and Prognosis of Ovarian Cancer

PRINCIPAL INVESTIGATOR: Douglas Taylor

CONTRACTING ORGANIZATION: University of Louisville  
Louisville, KY 40206

REPORT DATE: April 2012

TYPE OF REPORT: Annual

PREPARED FOR: U.S. Army Medical Research and Materiel Command  
Fort Detrick, Maryland 21702-5012

DISTRIBUTION STATEMENT: Approved for public release; distribution unlimited

The views, opinions and/or findings contained in this report are those of the author(s) and should not be construed as an official Department of the Army position, policy or decision unless so designated by other documentation.

REPORT DOCUMENTATION PAGE				Form Approved OMB No. 0704-0188	
Public reporting burden for this collection of information is estimated to average 1 hour per response, including the time for reviewing instructions, searching existing data sources, gathering and maintaining the data needed, and completing and reviewing this collection of information. Send comments regarding this burden estimate or any other aspect of this collection of information, including suggestions for reducing this burden to Department of Defense, Washington Headquarters Services, Directorate for Information Operations and Reports (0704-0188), 1215 Jefferson Davis Highway, Suite 1204, Arlington, VA 22202-4302. Respondents should be aware that notwithstanding any other provision of law, no person shall be subject to any penalty for failing to comply with a collection of information if it does not display a currently valid OMB control number. <b>PLEASE DO NOT RETURN YOUR FORM TO THE ABOVE ADDRESS.</b>					
1. REPORT DATE (DD-MM-YYYY) 01-04-2012		2. REPORT TYPE Annual		3. DATES COVERED (From - To) 1 APR 2011 - 31 MAR 2012	
4. TITLE AND SUBTITLE Exosomal microRNA Signatures in the Diagnosis and Prognosis of Ovarian Cancer				5a. CONTRACT NUMBER	
				5b. GRANT NUMBER W81XWH-10-1-0196	
				5c. PROGRAM ELEMENT NUMBER	
6. AUTHOR(S) Douglas Taylor  E-Mail: ddtaylor@louisville.edu				5d. PROJECT NUMBER	
				5e. TASK NUMBER	
				5f. WORK UNIT NUMBER	
7. PERFORMING ORGANIZATION NAME(S) AND ADDRESS(ES) University of Louisville Louisville, KY 40206				8. PERFORMING ORGANIZATION REPORT NUMBER	
9. SPONSORING / MONITORING AGENCY NAME(S) AND ADDRESS(ES) U.S. Army Medical Research and Materiel Command Fort Detrick, Maryland 21702-5012				10. SPONSOR/MONITOR'S ACRONYM(S)	
				11. SPONSOR/MONITOR'S REPORT NUMBER(S)	
12. DISTRIBUTION / AVAILABILITY STATEMENT Approved for Public Release; Distribution Unlimited					
13. SUPPLEMENTARY NOTES					
14. ABSTRACT Our original goal was to correlate exosomal miRNA profiles within circulating tumor-derived exosomes with cancer diagnosis, characterization of circulating tumor-derived vesicles and development of methodology for their specific isolation were essential for specific analyses of tumor-derived exosomal cargoes. Our discovery of exosomal microRNA in cancer patients focused on miRNAs, previously demonstrated in tumor biopsies or ovarian tumor cells. We have observed that while some miRNAs that are up-regulated with the tumor or also up-regulated in their exosomes, some tumor-up-regulated miRNAs are not up-regulated within exosomes. Further, certain miRNAs down-regulated within the tumor are up-regulated in exosomes. We demonstrate that miRNA signatures derived from ovarian tumor exosomes exhibit some miRNAs that are undetectable within the tumor. These findings demonstrate the highly selective nature of miRNA "packaging." Although the exosomal miRNA signatures for ovarian cancer patients appear to be similar regardless of stage, significant differences among early (Stage I and II) and late stage (Stage III) ovarian cancer were demonstrated: increase expression level and elevated expression of three specific miRNAs within exosomes. Exosomes from ovarian cancer patients were demonstrated to possess elevated levels of RNA, including the presence of specific long-noncoding RNA.					
15. SUBJECT TERMS Exosomes, microRNA, Diagnostic biomarkers, Ovarian Cancer					
16. SECURITY CLASSIFICATION OF:			17. LIMITATION OF ABSTRACT  UU	18. NUMBER OF PAGES  25	19a. NAME OF RESPONSIBLE PERSON USAMRMC
a. REPORT U	b. ABSTRACT U	c. THIS PAGE U			19b. TELEPHONE NUMBER (include area code)

**TABLE of CONTENTS**

<b>INTRODUCTION</b>	<b>4</b>
<b>KEY RESEARCH ACCOMPLISHMENTS</b>	<b>7</b>
<b>REPORTABLE OUTCOMES</b>	<b>8</b>
<b>Numeration and characterization of circulating vesicles</b>	<b>8</b>
<b>Improved exosome isolation (Immunotyping)</b>	<b>13</b>
<b>Association and selectivity of microRNA in circulating exosomes</b>	<b>15</b>
<b>Demonstration of lncRNA in tumor-derived exosomes</b>	<b>17</b>
<b>CONCLUSIONS</b>	<b>20</b>
<b>REFERENCES</b>	<b>23</b>

## INTRODUCTION

Despite progress made in the understanding and treatment of ovarian cancer, it remains the fourth leading cause of cancer-related deaths in women, resulting in more than 25,500 new cases and 15,310 deaths annually in the U.S.<sup>1,2</sup> Most women with ovarian cancer are diagnosed at an advanced stage, with 75% of cases diagnosed with extra-ovarian disease. This late diagnosis may reflect the inaccessibility of the ovaries and the lack of early symptoms.<sup>3</sup> The anatomical location of the ovaries results in minimal interference with vital structures or local irritation, making the diagnosis of ovarian cancer difficult, until regional and distant metastases have occurred.

Although ovarian cancer accounts for only a third of gynecologic cancers, it results in 55% of the deaths from gynecologic malignancies and 6% of all cancer deaths in women.<sup>4,5</sup> Long-term survival has not changed significantly in the last two decades, largely due to inadequacy of diagnostic approaches, which only detects well-established overt cancers. Stage I ovarian cancer can be cured in 90% of cases, while five-year survival for patients with advanced disease (Stage III and IV) is less than 21%. In comparison with other cancers associated with women, 73% of endometrial cancers, 55% of breast cancers and 50% of cervical cancers are diagnosed as Stage I, while only 23% of ovarian cancers are diagnosed at an early stage.<sup>6</sup> Thus, prospects for significant improvement in ovarian cancer survival reside in early diagnosis of disease.

The only biomarker currently approved for ovarian cancer detection is CA125 and its quantitation by ELISA has been the “gold standard” for detection of ovarian cancer, since its introduction in 1983.<sup>7</sup> Assessment of CA125 is typically used in disease management, both for disease detection as well as monitoring for disease recurrence; however, the use of CA125 is limited with regard to early stage cancer detection (sensitivity from 50–60%).<sup>8</sup> CA125 quantitation is only approved for and consistently proven for remission monitoring. CA125 is neither sensitive nor specific for *de novo* ovarian cancer detection, since it is elevated in >50% of women with stage I disease, although it is elevated in more than 80% of patients with advanced stage ovarian cancer. CA125 has poor specificity, which is shown by its elevation in association with benign and malignant breast and colon disease, peritoneal irritants, and benign gynecologic diseases, among others. Significant effort has been expended in the recent years for identifying potential markers that might substitute or complement CA125 in disease management or ultimately in the design of screening strategies.<sup>9</sup>

To address these problems, new technologies are being investigated. New strategies that facilitate proteomic analysis by dramatically simplifying the pre-analytical sample separation and coupling with mass spectrometry (MS) have been introduced for biomarker discovery research. Surface-enhanced laser desorption/ionization time-of-flight mass spectrometry (SELDI-TOF-MS) has received much attention for its use in resolving proteins in biological specimens by binding to biochemically distinct ProteinChip arrays. In LabCorp’s technology, 4 serum proteins are examined by ELISA, while Correllogic Systems and CIPHERgen Biosystems use mass spectrometry of 7 specific serum components or general peptide patterns in patient serum to define the presence of cancer. SELDI-TOF-MS profiling has been successfully used to differentiate ovarian, breast, prostate, and liver cancer from controls.<sup>10</sup> SELDI-TOF-MS profiling of serum was significantly better than the current standard serum biomarker CA125 at distinguishing patients with ovarian cancer from those with benign ovarian disease and from healthy controls.<sup>11</sup> Studies have shown that the selection of a combination of multiple proteins resolved by SELDI-TOF-MS may become a potential diagnostic approach. An effective screening test for ovarian cancer needs to achieve a high sensitivity and specificity and currently, different proteomic technologies as well as the computational analytic tools used to discern peaks generate different findings. These initial studies on SELDI-TOF-MS profiling insights are promising, and the concept is reproducible in a series of different backgrounds; however, translating this approach into a routine diagnostic test remains difficult.

Jacobs and Menon calculated that to be an effective screening test, an assay needs to achieve a minimum of 99.6% specificity.<sup>12</sup> To achieve this level of specificity, multiple components of the tumor’s characteristics will need to be incorporated into new diagnostic tests for effective detection because of the multifactorial nature of ovarian cancer. A drawback of mass spectrometry techniques is that some

samples of importance may be masked by more abundant proteins in the MS as well as in the analysis of the spectrometric output. Prepurification by a number of techniques such as high-performance liquid chromatography and positive or negative selection through affinity binding can remove particular groups of proteins. The greatest challenge in most current mass spectrometry approaches is the dynamic range rather than sensitivity. While removal of prevalent proteins or peptides can greatly increase the informational content that can be acquired from particular samples, prevalent proteins such as albumin can function as carriers of protein subsets of diagnostic significance. Additional studies with larger samples sizes and careful blinding of the independent validation sets are needed before any consideration of application of this platform for screening for ovarian cancer or any other indication should be considered.

One general characteristic of tumors is their ability to release or shed intact, vesicular portions of the plasma membrane (termed membrane fragments, membrane vesicles, microvesicles or exosomes), which was initially described by us.<sup>13</sup> Exosomes are described as microvesicles containing 5'-nucleotidase activity that are released from neoplastic cell lines. These small vesicles (50-100nm in diameter), which were present inside large multivesicular endosomes, contained transferrin receptors, a marker that is used to follow endocytosis and the recycling of cell-surface proteins, that had been internalized from the plasma membrane.<sup>14,15</sup> The precise mechanisms of exosome release/shedding remain unclear; however, this release is an energy-requiring phenomenon, modulated by extracellular signals. They appear to form by invagination and budding from the limiting membrane of late endosomes, resulting in vesicles that contain cytosol and that expose the extracellular domain of transferrin receptors at their surface. Using electron microscopy, studies have shown fusion profiles of multivesicular endosomes with the plasma membrane, leading to the secretion of the internal vesicles into the extracellular environment. The rate of exosome release is significantly increased in most neoplastic cells and occurs continuously.<sup>16</sup> Increased release of exosomes and their accumulation appear to be important in the malignant transformation process. In addition to cancer cells, the release of exosomes was also demonstrated to be associated with cells of embryonic origin (such as the placenta) and activated lymphoid cells.<sup>17-20</sup> Although extracellular shedding of exosomes occurs in other types of cells, under specific physiological conditions, the accumulation of exosomes from non-neoplastic cells is rarely observed, *in vivo*.<sup>17,21</sup> In contrast, exosomes released by tumor cells accumulate in biologic fluids, including in sera, ascites, and pleural fluids. Exosome release and its accumulation appear to be important features of the malignant transformation. Shed tumor derived exosomes do not mirror the general composition of the plasma membrane of the originating tumor cell, but represent 'micromaps,' with enhanced expression of tumor antigens.<sup>17,22</sup>

The release of exosomes appears to be important features of intercellular communication. Since released exosomes express molecules with biologic activity (such as Fas ligand, PD-1, MICA/B, mdrl, MMPs, CD44, and autoreactive antigens),<sup>23-26</sup> the ability of these microvesicles to modulate lymphocyte and monocyte functions have been analyzed in several models. It has been theorized that these released exosomes modulate lymphocyte functions by mimicking "activation induced cell death" (AICD).<sup>27,28</sup> Lymphoid cells appear to release exosomes following activation and these appear to play an essential role in immunoregulation, by preventing excessive immune responses and the development of autoimmunity.<sup>30</sup> It was postulated that exosome release by tumor cells is a re-expression of the fetal cell exosomes and that both constituted pathways to circumvent immunosurveillance.<sup>30</sup>

miRNAs are small endogenous noncoding RNA gene products about 22 nucleotides (nt) long that regulate gene expression in a sequence-specific manner and are found in diverse organisms. With >300 already identified, the human genome may contain up to 1,000 miRNAs. miRNA play key roles in regulating the translation and degradation of messenger RNAs through base pairing to partially complementary sites, predominately in the untranslated region of the message.<sup>31-33</sup> miRNAs are expressed as long precursor RNAs. Drosha, an RNase III endonuclease, is responsible for processing primary miRNAs in the nucleus and releasing ~70nt precursor miRNAs.<sup>34,35</sup> Drosha associates with the dsRNA-binding protein DGCR8 in human to form the microprocessor complex. Precursor miRNAs are

transported to the cytoplasm by exportin-5 and cleaved by the RNase III endonuclease Dicer, releasing 17–24nt mature dsmiRNA.<sup>36,37</sup> One strand of the miRNA duplex is subsequently incorporated into the effector complex RNA-induced silencing complex (RISC) that mediates target gene expression. Argonaute2, a key component of RISC, may function as an endonuclease that cleaves target mRNAs.

While the biological functions of most miRNAs are not yet fully understood, it has been suggested that the miRNAs are involved in various biological processes, including cell proliferation, cell death, stress resistance, and fat metabolism, through the regulation of gene expression.<sup>38</sup> As potential clinical diagnostic tools miRNAs have been shown to be important and accurate determinants for many if not all cancers.<sup>39</sup> Increasing evidence shows that expression of miRNA genes is deregulated in human cancer. The expression of miRNAs is highly specific for tissues and developmental stages and has allowed recently for molecular classification of tumors. To date, all tumors analysed by miRNA profiling have shown significantly different miRNA profiles compared with normal cells from the same tissue. Flow-cytometric miRNA profiling demonstrated that miRNA-expression profiles classify human cancers according to the developmental lineage and differentiation state of the tumors. Specific over- or underexpression has been shown to correlate with particular tumor types. miRNA overexpression could result in down-regulation of tumor suppressor genes, whereas their underexpression could lead to oncogene up-regulation. Using large-scale microarray analysis, cancer cells showed distinct miRNA profiles compared with normal cells with 36 of the 228 miRNA genes overexpressed and 21 downregulated in cancer cells versus normal cells.<sup>40</sup> Hierarchical clustering analyses showed that this miRNA signature enabled the tumour samples to be grouped on the basis of their tissue of origin. Genome-wide profiling studies have been performed on various cancer types, including CLL,<sup>41</sup> breast cancer,<sup>42</sup> glioblastoma,<sup>43</sup> thyroid papillary carcinoma,<sup>44</sup> hepatocellular carcinoma,<sup>45</sup> ovarian cancer,<sup>46</sup> colon cancer,<sup>47</sup> and endocrine pancreatic tumours.<sup>48</sup> In a study of 104 matched pairs of primary cancerous and non-cancerous ovarian tissue, 43 differentially expressed miRNAs were observed; 28 were downregulated and 15 were overexpressed in tumors.<sup>49</sup>

Statistical analyses of microarray data obtained by two different methods, significance analysis of microarrays (SAM) and prediction analysis of microarrays (PAM) from six solid tumours (ovarian, breast, colon, gastric and prostate carcinomas and endocrine pancreatic tumours), demonstrated a common signature composed of 21 miRNAs differentially expressed in at least three tumor types.<sup>50</sup> At the top of the list were miR-21, which was overexpressed in six types of cancer cells, and miR-17-5p and miR-191, which were overexpressed in five. As the embryological origin of the analysed tumors was different, the significance of such findings could be that these common miRNAs participate in fundamental signalling pathways altered in many types of tumor. Supporting the function of these genes in tumorigenesis, it was found that the predicted targets for the differentially expressed miRNAs are significantly enriched for those that target known tumor suppressors and oncogenes.<sup>51</sup> Furthermore, miR-21, the only miRNA overexpressed in all six types of cancer analyzed was shown to directly target the tumor suppressor PTEN, which encodes a phosphatase inhibiting growth and/or survival pathways. The function of PTEN is altered in advanced tumors of various types, including breast, ovarian, gastric and prostate.<sup>52</sup>

## KEY RESEARCH ACCOMPLISHMENTS

Over the past 12-month grant period, these investigations have generated multiple accomplishments leading to significant improvements of ovarian cancer diagnostic and prognostic markers.

1. Quantitative and quality characterization of circulating vesicles in ovarian cancer patients
2. Development of methodology for specific isolation of tumor-derived circulating exosomes
3. Expanded analyses of tumor-derived exosomal microRNA expression
4. Demonstration of selective release of specific microRNAs within the tumor exosomes
5. Association of specific microRNAs with the presence of late stage ovarian cancer
6. Discovery of tumor-derived exosomal long-noncoding RNA

As the original Aim 1 was to define the utility of exosomal miRNA profiles as diagnostic biomarkers by correlating specific miRNAs associated with circulating tumor-derived exosomes with diagnosis (stage and grade), achievement of Items 1 and 2 were essential to enable the specific analyses of tumor-derived exosomes and their contents from those exosomes derived from normal cells within the peripheral circulation (ie, reduction of “noise” to enhance the signal to noise ratio). We have continued to increase the number of ovarian cancer patients at each stage evaluated to define the microRNA signatures of the tumors (Item 3). Our original discovery of exosomal microRNA in cancer patients focused on a small number of miRNAs that previous groups demonstrated to be diagnostic using tumor biopsies or cultured ovarian tumor cells; however, we have observed that while some miRNAs that are up-regulated with the tumor or also up-regulated in their exosomes, some tumor-up-regulated miRNAs are not up-regulated within exosomes (Item 4). In addition, we observed that certain miRNAs that exhibit down-regulation within the tumor are up-regulated in exosomes. We have further investigated this finding and demonstrate that in many cases, miRNA signatures derived from ovarian tumor cell exosomes exhibit some miRNAs that are undetectable within the tumor. Our findings in multiple ovarian tumor cell lines demonstrate commonality in these miRNAs. This finding is in addition to cellular down-regulated miRNAs being up-regulated in exosomes derived from the same cells. These findings demonstrate the highly selective nature of miRNA “packaging” into exosomes. Based on these findings, previous data are being re-evaluated to incorporate those miRNAs (not appearing in the tumor cells) into the “diagnostic” signature. Although the exosomal miRNA signatures for ovarian cancer patients appear to be similar regardless of stage, work within the past 12 months has demonstrated significant differences among early (Stage I and II) and late stage (Stage III) ovarian cancer: general increase expression level and the elevated expression of three specific miRNAs within exosomes (Item 5).

While not included with the original objectives of this study, our work demonstrated that exosomes from ovarian cancer patients possessed elevated levels of RNA (less 400 nt). Our proposal focused on the miRNA populations. However, during the past 12 months, we further analyzed this “larger” RNA material. We demonstrated the presence of specific long-noncoding RNA (Item 6).

Summaries of the findings for these six key research accomplishments are presented on the following pages.



## REPORTABLE OUTCOMES

### NUMERATION AND CHARACTERIZATION OF CIRCULATING VESICLES IN OVARIAN CANCER

#### Circulating vesicle concentration and size distribution by Nanoparticle Tracking analysis (NTA):

To define the total numbers of circulating vesicles and their size distribution in clinical specimens, unfractionated sera from ovarian cancer patients, patients with benign disease and female controls were diluted in PBS (1:50-1:100) and applied directly to the sample chamber of the Nanosight LM10 (Figure 1). Patients with ovarian cancer exhibited an approximately 4-fold increase in the level of total circulating vesicles. The size distribution of these unfractionated vesicles from cancer patients ranged from approximately 50 to 300nm in diameter. Patients with benign disease and controls exhibited a similar size range; however, they possessed a greater percentage of vesicles within the 200-300nm range (versus cancer).

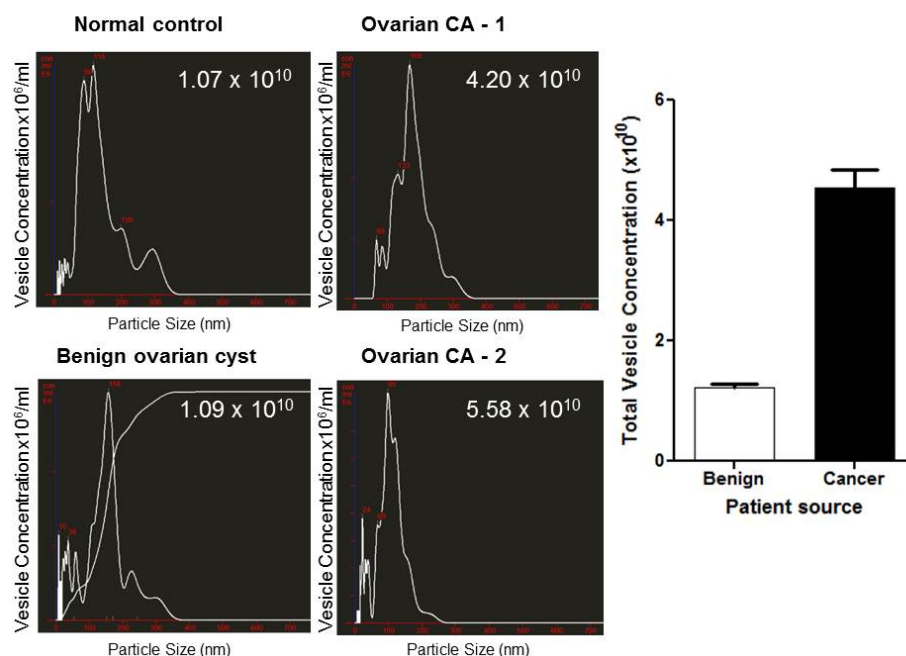


**Figure 1: NTA profile of unfractionated circulating vesicles in representative analyses of normal female controls, patients with benign ovarian disease and patients with ovarian cancer.** Sera were diluted in PBS and analyzed using a Nanosight LM10. Inset values represent the total number of vesicles counted/ml. The bar graph presents the mean and standard deviation of the vesicles concentrations for patients with benign and malignant ovarian disease.

**Size and phenotype characterization of chromatographically isolated vesicles:** Over the past 30 years, we have developed and refined an isolation procedure combining differential centrifugation and size exclusion chromatography. The use of high exclusion limit agarose-based gel has been previously demonstrated to generate a vesicle population consistent with those derived from the more labor-intensive sucrose density gradient centrifugation followed by ultracentrifugation. Fractionation of sera on Sepharose 2B resulted in two primary peaks of material (Figure 2A): a void volume and a retained peak. The void volume consists of material exhibiting a molecular weight greater than 50 million Daltons. The individual fractions of the void volume were examined by the Nanosight LM10 and NTA software. Fractions 15, 16, and 17 contained the peak of the void volume. NTA demonstrated a very narrow size range of vesicles (Figure 2B). Fraction 15 contained vesicles ranging from 50-200nm with a primary peak at 94nm (mode = 94nm, mean = 108, SD = 30nm). Fraction 16 exhibited vesicles also ranging from 50-200nm, but the primary peak appeared at 89nm (mode = 89nm, mean = 95nm, SD = 32nm). Fraction 17 consisted on vesicles ranging from 50-200nm with two principal vesicle peaks at 84nm and 108nm (mode = 84, mean = 109, SD = 30). The majority of the vesicles within Fractions 15, 16, and 17 falls within the 50-100 size range previously described for exosomes.



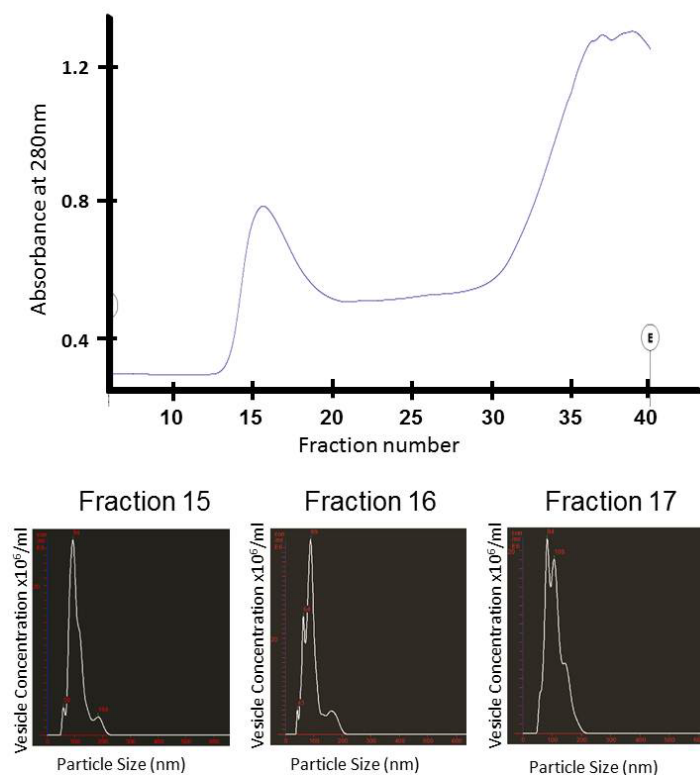


**Figure 2: Chromatographic isolation of circulating extracellular vesicles.** **Panel A:** A representative chromatogram of a serum sample obtained from ovarian cancer patient TB08-36 fractionated using a 2% agarose-based size exclusion gel. The peak containing exosomes appears in the void volume. **Panel B:** The three fractions corresponding to the void volume of the column were diluted in PBS and analyzed by NTA using a Nanosight LM10.

**Western immunoblotting of chromatographic isolated vesicles:** To identify the general distribution of proteins within the vesicular fractions, SDS-PAGE of each chromatographic fraction visualized by protein staining confirmed the similarity of the protein make-up of fractions 15, 16, and 17 (Figure 3A). Western immunoblotting of the individual fractions for specific markers claimed to be associated with either exosomes or microvesicles (Figure 3B). The tetraspanin, CD63, is defined as specific for exosomes, while CD154 (CD40 ligand) has been defined as specific for microvesicles. Western immunoblot analysis of the individual chromatographic fractions demonstrated the co-expressions of CD63 and CD154. While additional later fractions exhibiting elevated levels of CD40L, the void volume peak fractions exhibit the same profile for both CD63 and CD40L. The mutant EGFRvIII, generally considered to be associated with the plasma membrane of cancer cells also appeared to be associated with these void volume vesicles. Thus, while these vesicles are within the classic size range of exosomes, they exhibit markers previously defined as markers of exosomes and microvesicles [14]. Further, the presence of EGFRvIII demonstrates the tumor origin of these vesicles [27]. Similar analyses of vesicles from patients with benign ovarian disease demonstrated CD63-positive vesicles, but the absence of EGFRvIII (Figure 3C).

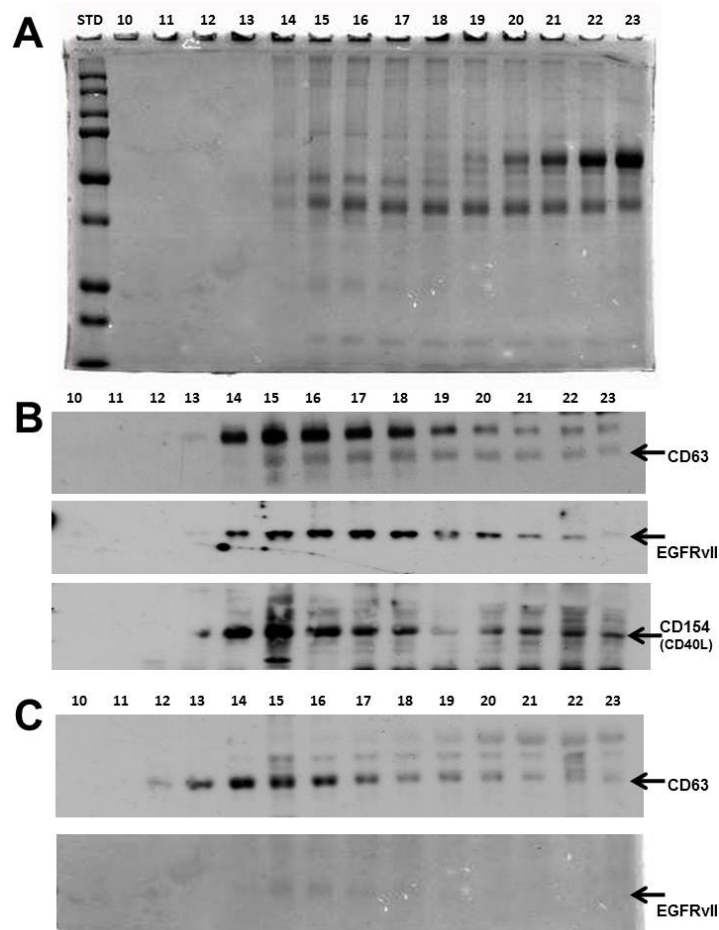


**Figure 3: Electrophoretic analyses of the chromatographic fractions from ovarian cancer patient TB08-36 and patient with benign adenoma. Panel A:** The separation of proteins from the chromatographic fraction on SDS-PAGE followed by total protein staining with Imperial Purple. Imperial purple stained 10% **SDS-PAGE analysis of a comparable amount of proteins (25µg).** **Panel B:** Western immunoblot evaluation of published markers of exosomes (CD63), microvesicles (CD154) and tumor origin (EGFRvIII) in vesicles isolated from patient TB08-36. **Panel C:** Western immunoblot evaluation of published markers of exosomes (CD63) and tumor origin (EGFRvIII) in vesicles isolated from patient with benign disease. Chromatographically derived vesicles (25µg protein) were separated on a 10% SDS-PAGE, transferred to nitrocellulose membranes, incubated with anti-CD63, anti-CD154, or anti-EGFRvIII antibodies.

**Comparison of sizing methodologies (NTA, SPA, DLS versus EM):** NTA, submicron analysis (SPA) and dynamic light scattering were compared with electron microscopic analysis of vesicles. For electron microscopy, the size distribution of vesicles was determined by measuring their diameters directly from electron micrographs of ultracentrifuge pellets (Figure 4A). NTA gave a vesicle size distribution from 50 to 175 nm with a mean = 100nm, mode = 87 and SD = 28 (Figure 4B). Analysis of the same vesicle preparation by DLS indicated a mean diameter of  $125.3 \pm 1.9$ nm (Figure 4C), while the submicron particle analysis indicated a range of 80 to 120nm (Figure 4D). These data are further summarized in Table 1. Although the area of the electron microscopy image selected contains vesicles between 50-100nm, EM has been shown to underestimate the size of vesicles. Further, vesicles larger than 100nm are clearly visible in multiple EM fields and the real size distribution of the entire vesicle population is not assessable. Thus, vesicle size ranges defined by EM tend to be subjective. DLS and SPA, while providing an objective size distribution of the entire vesicle population, do not define the concentration of the vesicles.

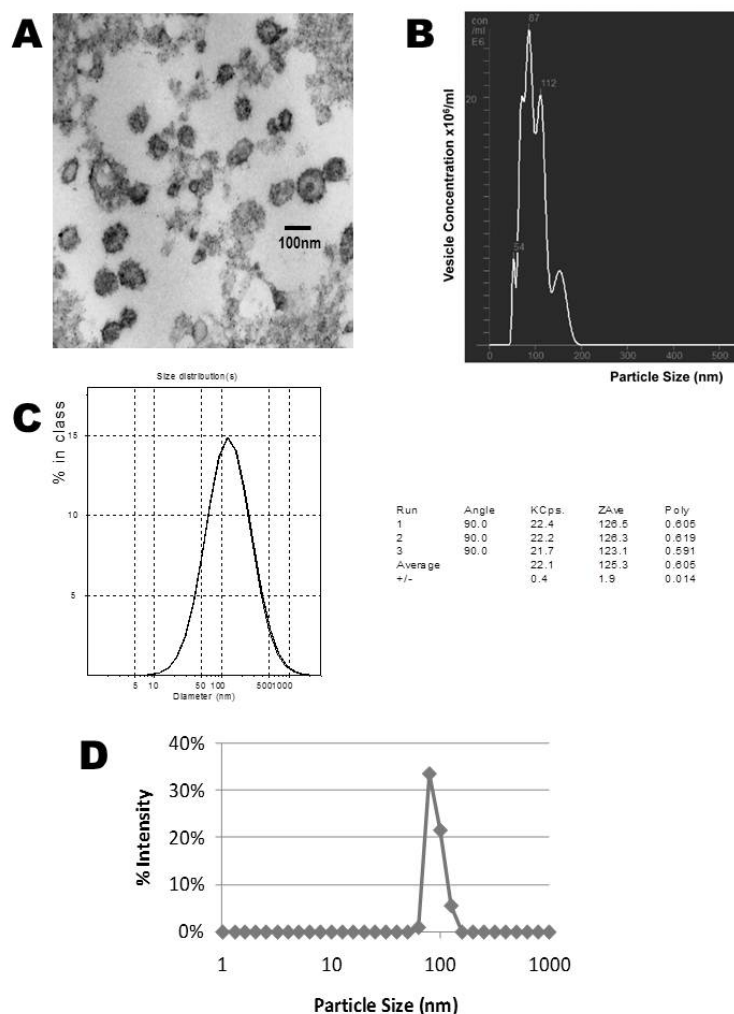


**Figure 4: Comparison of vesicle analyses by electron microscopy (A), NTA (B), DLS (C) and submicron particle analysis (D).** EM images reveal the presence of nano-sized vesicles with a circular shape. Scale bar, 100 nm (original magnification x45K).

**Phenotype of cell-derived vesicles:** A major limitation of DLS and SPA, as well as standard NTA, is that while they can objectively define the vesicle size range, they cannot define the “phenotype” of these vesicles. Using the NanoSight LM10 equipped with the 405-nm blue-violet laser and more sensitive camera to detect fluorescent particles, quantum dots attached to antibodies can be used identify specific subsets of vesicles. The instrument was initially calibrated using 100nm and 200nm fluorescent beads, which can be easily discriminated. Antibodies reactive with either CD63 (exosomes marker) or EpCAM (marker of vesicles derived from epithelial tumors) were conjugated with quantum dots. The labeled vesicle samples were analyzed on the NanoSight LM10, first in light scatter mode and then in fluorescence mode. Figure 5, Panel A shows the NTA profile in light scatter mode and then fluorescence for CD63 (Panel B) and EpCAM (Panel C). The size ranges of the CD63-labeled vesicles are similar, with peaks in the region of 100nm and 180nm whether measured in light scatter or fluorescence mode. The presence of EpCAM on the various size ranges of vesicles indicates their tumor origin. Vesicles both larger and smaller than 100nm exhibit CD63, the marker for exosomes, thus the published definition of exosomes as ranging only from 50-100nm may not be accurate.

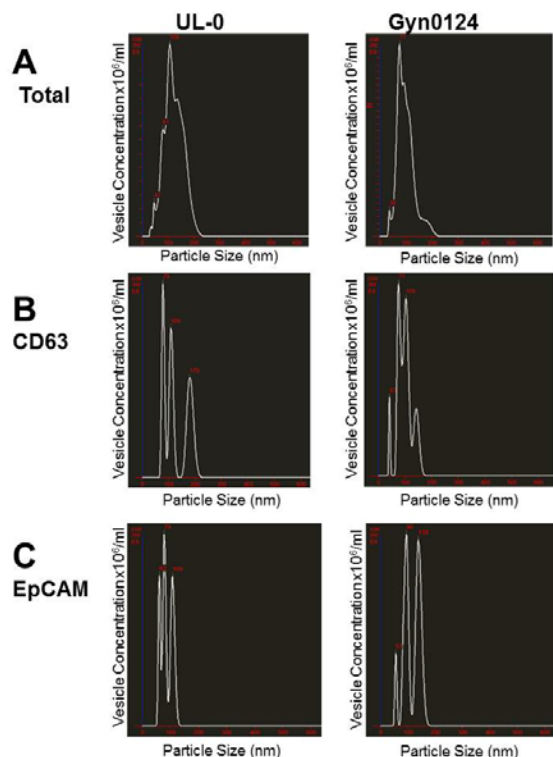


**Figure 5: Combination of NTA and fluorescent antibodies to characterize the phenotypes of chromatographically isolated vesicles from two ovarian cancer patients.** Vesicle suspensions were incubated with either Qdot-labeled anti-CD63 or Qdot-labeled antiEpCAM. These vesicles were then examined in light scattering mode to define total vesicle size distribution (**Panel A**) or in fluorescence mode to define CD63-positive vesicles (**Panel B**) or EpCAM-positive vesicles (**Panel C**).

**Analysis of disrupted cell-derived vesicles:** Vesicles were chromatographically isolated from ovarian cancer patients and diluted 1:100 in PBS. The sample presented in Figure 6A was the NTA total of untreated vesicles, while Panel B presents the same sample treated with 0.5% Triton X100 for 5 minutes at room temperature and reanalyzed under the same conditions. Based on NTA, the total number of particles was diminished approximately 10-fold. Particle size analysis was further performed using Coulter Model N4 Plus particle size analyzer in PBS at room temperature (SDP analysis, 17 bins in the range from 1-1000nm at 90 degrees) using weight analysis. The sample in Figure 6C presents the SPA distribution of the same sample. The values observed ranged from 80-120nm. Panel D was the same sample treated with 1% Tween 20 for 5 minutes at room temperature and reanalyzed in the same conditions. Based on SPA, the apparent weight average size of the particles shifted from 100 to ~10 nm (range 5-20 nm).

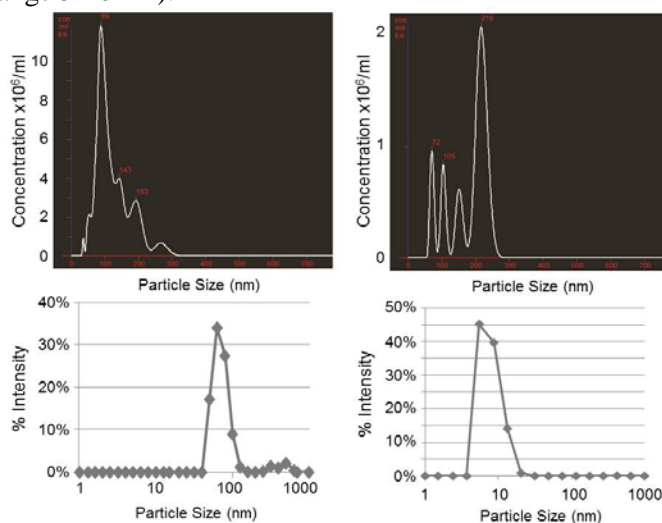


**Figure 6: Disruption of light scattering defined particles by non-ionic detergents.** The size distributions of chromatographically isolated vesicles were analyzed by either NTA (**A**) or submicron particle analysis (**C**). The same vesicles suspension was treated with either 0.5% Triton X-100 (**B**) or 1% Tween 20 (**D**) for 5 minutes at room temperature and re-analyzed. Treatment with non-ionic detergents disrupted the vesicles, either reducing the number and size under NTA or producing a size shift by SPA.

## IMPROVED EXOSOME ISOLATION (IMMUNOTYPING)

While immune cell functions are impaired in most ovarian cancer patients, as defined by the failure to eradicate the tumor, studies suggest immune recognition of tumor antigens remains intact, based on the presence of tumor-reactive IgG, including patients with melanoma, lung, breast, head and neck and ovarian cancers. Malignant diseases are associated with the induction of humoral immunity that is characterized by the generation of reactive IgG against a wide range of tumor-associated antigens (Th2 response). Genetic analyses of tumor cells derived from ovarian cancer patients have demonstrated alterations (mutations or amplifications) in specific genes, including oncogenes, tumor suppressor genes, and proliferation-associated genes. Studies in our laboratory, as well from other groups, have demonstrated a link between cancer-altered genes and development of reactive IgG against their protein products. The actual role of circulating tumor-reactive IgG is unclear; however, they have been demonstrated to correlate with poor prognosis and survival. While the use of tumor-reactive IgG as a potential diagnostic and/or prognostic tool has been investigated over the past decade, to date this work has primarily identified components with shared expression in non-neoplastic tissue and has failed to define antigenic targets exhibiting ubiquitous expression in cancers. These limitations result, in large part, from the use of wild-type recombinant proteins or products of tumor-derived genes translated in non-mammalian cells as targets to define immunoreactivity. The power of utilizing the autologous humoral response is its ability to define both major (mutations, splice variants) and minor alterations (overexpression, altered post-translational processing), which might lead to either altered antigenic appearance or aberrant association with other cellular components resulting in the induction of humoral responses. While the mechanisms underlying the induction of a humoral response appears to be multifaceted: alterations (mutations and post-translational modifications), overexpression, ectopic expression, subcellular compartment translocations, splice variant products, or errors in proteolytic processing of certain proteins have been demonstrated to elicit immune responses in cancer patients. Autoantibody responses to antigens broadly expressed in normal and cancer tissues appears to be attributable to tumor-specific mutations or post-translational modifications.

We hypothesize that by selectively capturing tumor-derived exosomes in blood samples, we can determine in real time the phenotypic state of tumors in individual patients. Cell derived vesicles can be released from many cell types; however, their accumulation within the peripheral circulation appears to be elevated 3-4-fold in cancer patients; however, only a fraction of these are produced by the tumor. Exosomes can be isolated from the peripheral circulation of these patients by high exclusion agarose chromatography. Sera samples (1ml) were separated on Sepharose 2B, monitoring elution at 280nm. The void volume fractions were pooled and added to the upper chamber of a Protein G spin column. The pooled vesicle fraction was incubated with the Protein G gel for 30 minutes at room temperature. The spin column was then centrifuged for 10 seconds at 800rpm and the flow-through collected. The Protein G spin column was washed with 1ml of TBS and re-centrifuged. This flow-through was combined with the first. The Protein G-spin column was then acidified by addition of 0.5ml 0.1M glycine-HCl, pH 2.5. The mixture was incubated for 20 minutes at 4°C and then centrifuged at 800rpm. After centrifugation, the lower chamber contained circulating exosomes isolated based on bound IgG. The eluted exosomes fraction was analyzed quantitatively and qualitatively.

Based on this immunoaffinity approach, we have demonstrated that tumor-derived exosomes are released into the blood and are present at  $\sim 2-5 \times 10^{10}$ /ml in the peripheral circulation of ovarian cancer patients. We have also demonstrated that exosomal protein profiles from tumor-derived plasma exosomes contain approximate representations of the proteome of the original tumor cell. This vesicular material from cancer patients was examined using a Nanosight LM10 instrument to confirm their size distribution. Isolation of tumor-specific exosomes by our immunoaffinity method based on Protein G beads revealed a subpopulation of vesicles.



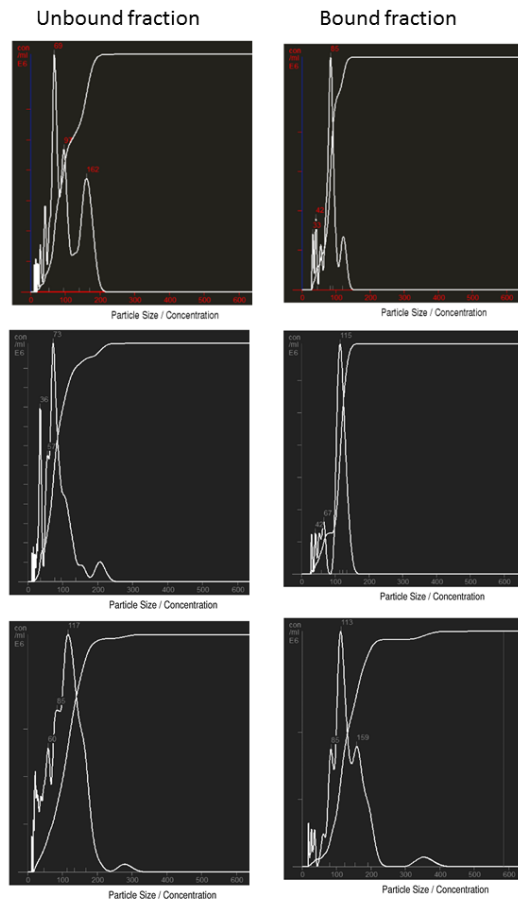
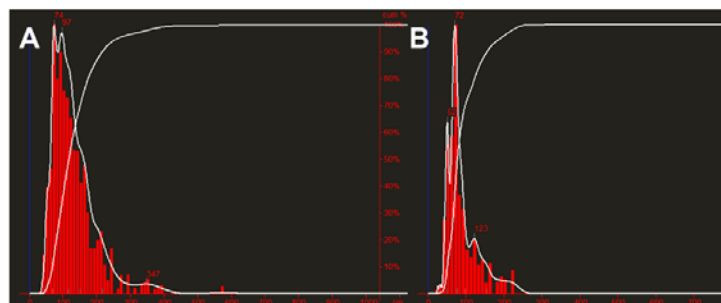


**Figure 7:** Nanosight tracking profile of sera derived vesicles from ovarian cancer patients. Chromatographically isolated vesicles were incubated with immobilized Protein G. The vesicle fraction not binding to the Protein G is shown as “UNBOUND.” The Protein G-binding vesicles were eluted with 0.1M glycine-HCl, neutralized with Tris base and are presented as “Bound.”

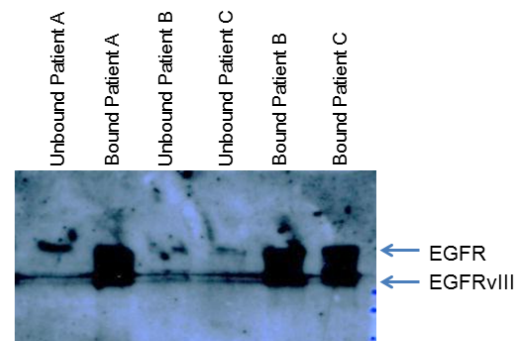
Isolation of tumor-specific exosomes by our proprietary immunoaffinity method based on Protein G beads revealed a subpopulation with the peak at 72nm. After separation based on Protein G binding, the bound exosomes were eluted and the number of bound vesicular particles was also determined by the



**Results**  
Mean: 134 nm  
Mode: 74 nm  
Concentration:  $2.35 \times 10^{11}$  particles/ml

Size distribution of circulating tumor derived exosomes from ovarian cancer ascites defined by the Nanosight LM10. Panel A presents the distribution of total circulating vesicular populations. Panel B presents the distribution of vesicular population by isolated from the circulating vesicles demonstrating the separation of a specific subpopulations.

**Results**  
Mean: 93 nm  
Mode: 72 nm  
Concentration:  $2.46 \times 10^{10}$  particles/ml

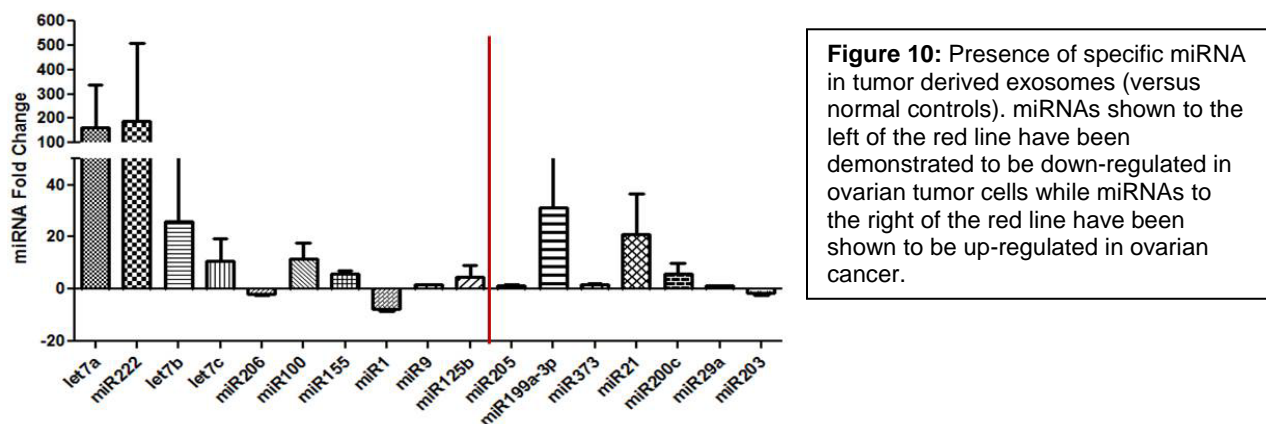


Enrichment of tumor-specific marker, EGFRvIII, based on selection by autoreactive IgG

Nanosight analysis, demonstrating the presence of  $2.46 \times 10^{10}$  vesicles/ml. The enrichment of a tumor-specific vesicle population was confirmed by the enhanced expression of the tumor marker, EGFRvIII (defined by Western immunoblotting).

### ASSOCIATION AND SELECTIVITY OF MIRNA IN CIRCULATING TUMOR EXOSOMES

Initially, miRNA was isolated from circulating tumor-derived exosomes using mirVana isolation kit. This total small RNA fraction was utilized for miRNA profiling as defined by qRT-PCR microarray analysis. Initial analyses were performed by cancer-specific arrays from SABiosciences. The small RNA-enriched fraction was extracted from the isolated exosomes. Using specific primers, presence and expression level of mature miRNAs was analyzed by TaqMan miRNA Assay (Applied Biosystems) under conditions defined by the supplier. LMW RNA was isolated from exosomes isolated from 1ml of sera using the mirVana miRNA Extraction Kit and quantified by the RiboGreen kit. Single-stranded cDNA will be synthesized from 5.5ng of total RNA in 15 $\mu$ l reaction volume by using the TaqMan MicroRNA Reverse Transcription Kit (AB). The reactions will be incubated first at 16°C for 30 min and then at 42°C for 30 min. The reactions will be inactivated by incubation at 85°C for 5 min. Each cDNA generated will be amplified by quantitative PCR by using sequence-specific primers from the TaqMan microRNA Assays Human Panel on a Agilent M3005P. The 20 $\mu$ l PCR mix will include 10 $\mu$ l of 2 $\times$  Universal PCR Master Mix, 2 $\mu$ l of each 10 $\times$  TaqMan MicroRNA Assay Mix and 1.5 $\mu$ l of reverse transcription (RT) product. The reactions will be incubated at 95°C for 10 min, followed by 40 cycles of 95°C for 15 s and 60°C for 1 min. The threshold cycle ( $C_T$ ) is defined as the fractional cycle number at which the fluorescence passes the fixed threshold (0.2). All signals with  $C_T \geq 37.9$  will be manually set to undetermined. The relative quantity (RQ) of the target miRNAs will be estimated by the  $\Delta C_T$  study by using as reference (exogenous control) for each preparation. Each sample will be run in duplicate and each PCR experiment will include two non-template control wells. From this analyses, exosomal miRNAs that were previously reported to be specifically up-regulated in ovarian cancer cells were examined (Figure 10). Similarly, those exosomal miRNAs shown to be specifically down-regulated were examined.



Within the Cancer qRT-PCR miRNA array, 10 miRNAs have been reported to be up-regulated. Of these, 8 miRNAs were also up-regulated by more than 2-fold within exosomes; however, 2 miRNAs (miR-206 and miR-1) were down-regulated in tumor-derived exosomes. Within the Cancer miRNA qRT-PCR array, 7 miRNAs have been reported to be down-regulated in ovarian tumor cells. Of these 7 miRNAs, only 1 expressed a down-regulation of more than 2-fold (miR-203). Six of these miRNAs were up-regulated by more than 2-fold within exosomes and the other 6 exhibited greater than a 2-fold elevation. These results suggest that certain specific miRNAs are “packaged” within exosomes, with little detectable miRNAs remaining within the originating cells. In contrast, miRNAs up-regulated within the tumor cells appear to be mirrored by their expression within the exosomes.

One objective of this study was to define miRNA signatures that might differentiate early and late stage ovarian cancer. For these studies, serum specimens of patients with Stage I, II or III serous papillary adenocarcinoma of the ovary were evaluated. The small RNA-enriched fraction was extracted from the isolated exosomes. Using specific primers, presence and expression level of mature miRNAs was



analyzed by TaqMan miRNA Assay (Applied Biosystems) under conditions defined by the supplier. LMW RNA was isolated from exosomes isolated from 1ml of sera using the mirVana miRNA Extraction Kit and quantified by the RiboGreen kit. Single-stranded cDNA will be synthesized from 5.5ng of total RNA in 15µl reaction volume by using the TaqMan MicroRNA Reverse Transcription Kit (AB). The reactions will be incubated first at 16°C for 30 min and then at 42°C for 30 min. The reactions will be inactivated by incubation at 85°C for 5 min. Each cDNA generated will be amplified by quantitative PCR by using sequence-specific primers from the TaqMan microRNA Assays Human Panel on a Agilent M3005P. The 20µl PCR mix will include 10µl of 2× Universal PCR Master Mix, 2µl of each 10× TaqMan MicroRNA Assay Mix and 1.5µl of reverse transcription (RT) product. The reactions will be incubated at 95°C for 10 min, followed by 40 cycles of 95°C for 15 s and 60°C for 1 min. The threshold cycle ( $C_T$ ) is defined as the fractional cycle number at which the fluorescence passes the fixed threshold (0.2). All signals with  $C_T \geq 37.9$  will be manually set to undetermined. Using the Cancer miRNA qRT-PCR array, while the heat maps were similar across stages, the advanced ovarian cancer patients generally expressed enhanced miRNA expression (Figure 11). This elevated expression within exosomes from Stage III ovarian cancer patients was also observed with the scatter plot (Figure 12).

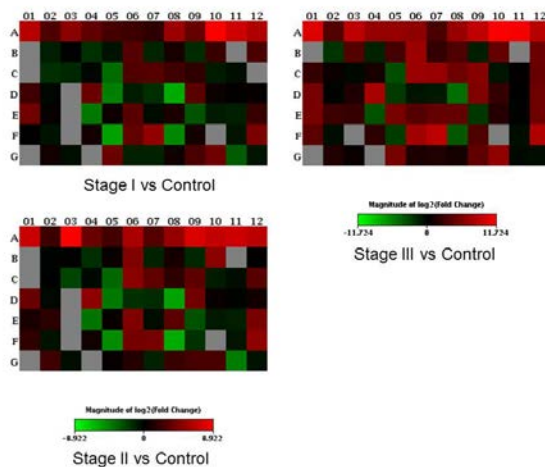


**Figure 11:** Heat maps of microRNA arrays examining the expression of miRNA in exosomes isolated from ovarian cancer patients at various stages versus controls.

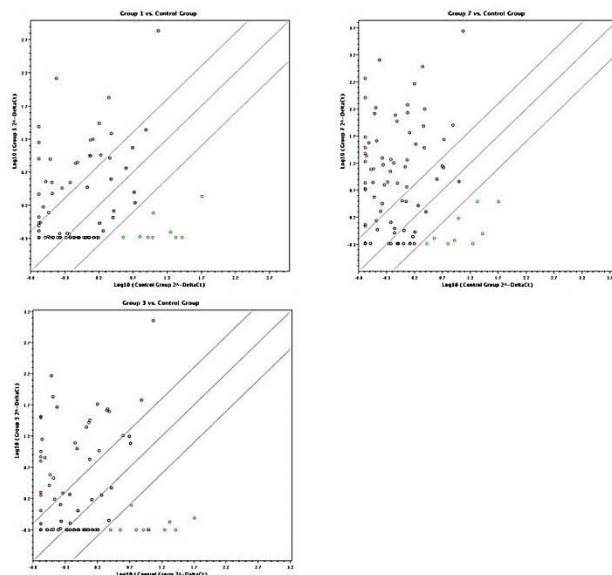


**Figure 12:** Scatter plot of miRNA expression associated with exosomes from Stage I (Group 1), Stage II (Group 2) or Stage III (Group 3) ovarian cancer

Comparisons between these populations of exosomes derived from cancer patients were not significantly different for most of these miRNAs. The similarity across the stages of ovarian cancer may result from the standardization of starting exosomal small RNA quantities and the normalization of the resulting array data. Despite this standardization and normalization, the profiles obtained with exosomal miRNA from patients with advanced ovarian cancer (Stage III) exhibited some distinct differences (Figure 13). While exosomes derived from all patients with ovarian cancer exhibited similarities, these were distinguished from patients without cancer (both controls and benign disease) and patients with advanced ovarian cancer exhibit a unique signature.

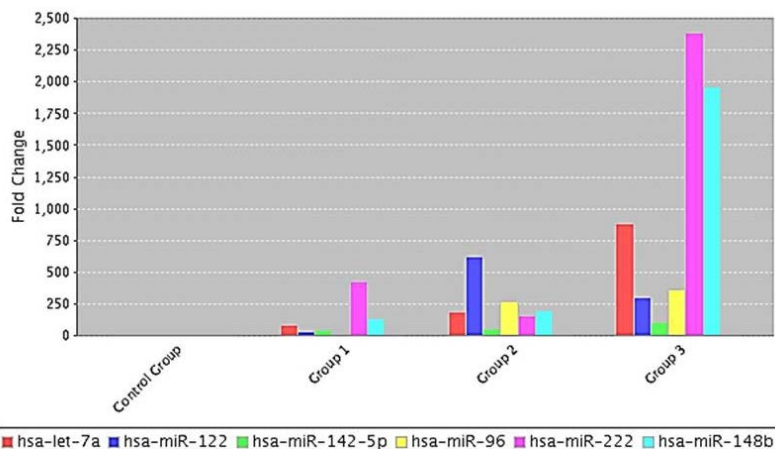


**Figure 13:** Association of specific miRNAs with stages of ovarian cancer. Control lane represents miRNA isolated from normal controls. Group 1 represents exosomal miRNAs isolated from Stage I, Group 2 corresponds to Stage II and Group 3 to Stage III.

## DEMONSTRATION OF lncRNA IN TUMOR-DERIVED EXOSOMES

Long noncoding RNAs (lncRNAs) are master regulators of pluripotency, differentiation, body axis patterning and promoting developmental transitions. LncRNAs represent non-coding RNA that are greater than 200 nucleotides in length. Dysregulation of lncRNA expression has been shown to be associated with a wide range of defects in development and pathologies. Currently lncRNAs have been found to exhibit a wide range of functions ranging from signaling, serving as molecular decoys, guiding ribonucleoprotein complexes to specific chromatin sites and also participating as scaffolds in the formation of complexes.

- **Signaling:** The transcription of certain lncRNAs is very tissue and temporal specific. Their expression can be in response to certain stimuli, such as cellular stress and temperature. Thus, lncRNAs can serve as molecular signals and can act as markers of functionally significant biological events.
- **Decoys:** The molecular decoy type of activity takes place when specific lncRNAs are transcribed and then bind to and titrate away protein factors. Decoy lncRNAs can "sponge" protein factors such as transcription factors and chromatin modifiers. This leads to broad changes in the cell's transcriptome.
- **Guides:** lncRNAs can be molecular guides by localizing particular ribonucleoprotein complexes to specific chromatin targets. This activity can cause changes in gene expression either in cis (on neighboring genes) or in trans (distantly located genes) that cannot be easily predicted by just the lncRNA sequence itself.
- **Scaffolds:** Assembly of complex protein complexes can be supported by lncRNAs, linking factors to together to form new functions. LncRNAs function as molecular scaffolds regulating histone modifications and influence the epigenetic programs of the transcriptome. Some lncRNAs

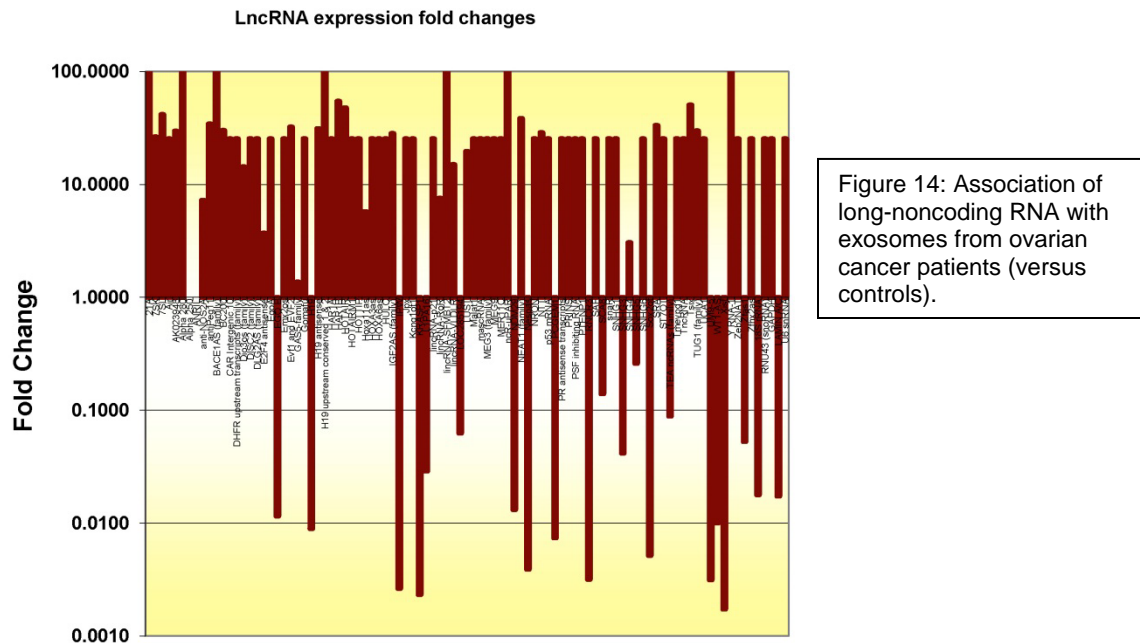
possesses different domains that bind distinct protein factors that altogether, may impact transcriptional activation or repression.

While lncRNAs have been identified within cells, we have demonstrated their presence within circulating exosomes. The presence of exosomal lncRNA is demonstrative of the presence of ovarian disease, with specific patterns distinguishing benign and malignant pathologies.

This study analyzed lncRNA within ovarian tumor cell lines and in vitro released exosomes, as well as within exosomes derived from patients with serous papillary adenocarcinoma of the ovary. For ovarian tumor cells, cells were grown in HyClone Serum-free media (SFM). After 3 days, media was removed and centrifuged at 400xg to remove cells and at 10,000xg to remove cell debris. The supernatant was concentrated 10-fold and microvesicles isolated by chromatography using Sepharose 2B. The void volume (vesicle fraction) was treated with Trizol to isolate total RNA. The total RNA fraction was analyzed for specific lncRNAs using the lncRNA profiler qPCR array (Systems Biosciences). Similarly, the tumor cells were directly extracted with Trizol to isolate the RNA fraction and the lncRNAs were analyzed using the lncRNA profiler array. For patient sera, vesicles were isolated using ExoQuick (Systems Biosciences) from 1ml samples of sera obtained from patients with ovarian cancer (n=8) by the manufacturer's instructions. The pelleted vesicles were extracted with Trizol to isolate the RNA fraction and the lncRNAs were analyzed using the lncRNA profiler array. As a control, exosomes were isolated from pooled normal human sera by ExoQuick and total RNA was isolated by Trizol and analyzed in parallel.

Exosomes isolated from the media of cultured tumor cells contain RNA populations. One population identified here was lncRNA. Comparison of lncRNA profiles between tumor cells and their released exosomes reveal selectivity on the lncRNAs appearing in the exosomes. Of the 90 lncRNAs examined, 3 exhibited greater than 10-fold increase in the exosome population. As lncRNA are defined with specific regulatory activity, representative lncRNAs were compared between the cells and their released exosomes. For lncRNAs exhibiting epigenetic silencing, the CT value of ANRIL in cells was 23.80 compared to 26.44 in exosomes. Among lncRNAs exhibiting splicing regulation, the CT value of MALAT-1 in cells was 31.84 compared to 32.85 in exosomes. For lncRNAs regulating apoptosis, the CT value of GAS-5 in cells was 31.72 compared to 29.86 in exosomes. Within lncRNAs expressing translation control, the CT value of BACE1AS in cells was 34.14 compared to 34.86 in exosomes.

lncRNAs were detected within the exosomes isolated from the peripheral circulation of patients. While exosomal lncRNAs can be detected in both cancer patients and normal controls, the lncRNA profiles of cancer patients exhibit profiles distinct from normal (Figure 14). Of the 90 lncRNA analyzed, an increase of greater than 20-fold was observed in 58 lncRNAs in cancer patient-derived exosomes (versus control). In contrast, a decrease of 10-fold or greater was observed in 20 lncRNAs in cancer patients versus controls. Among lncRNAs exhibiting epigenetic silencing, HOTAIR exhibited a 42.85-fold increase in cancer-derived exosomes versus controls. In lncRNAs exhibiting splicing regulation, MALAT-1 was increased 24.7-fold in tumor-derived exosomes compared with controls. For lncRNAs regulating apoptosis, GAS-5 was elevated 30.4-fold in cancer patient-derived exosomes versus controls. Within lncRNAs expressing translation control, BACE1AS was elevated 10,262-fold in patient exosomes versus controls.



LncRNAs contribute to genetic regulatory roles, including imprinting, epigenetic regulation, cell cycle control, nuclear and cytoplasmic trafficking, transcription, splicing, cell differentiation and apoptosis. Within tumors, the misexpression of lncRNAs contributes to cancer development and progression. Cancer patients exhibit a significant increased level of circulating vesicles in the range of 50-200nm, which exhibited markers confirming their exosome origin. These exosomes contain lncRNA and their profiles were distinct from non-cancer controls. Some lncRNAs, such as MALAT-1 (metastasis-associated in lung adenocarcinoma transcript) were identified in ovarian cancer and demonstrated to be critical in early stage development. Here we demonstrate the elevation of this lncRNA in exosomes from ovarian cancer patients. The stability of exosomes in the peripheral circulation and the unique profile of lncRNAs suggest their ideal utility as a diagnostic biomarker.

## CONCLUSIONS

Cell-derived vesicles and exosomes are potential markers of human disease. This could include the identification of elevated circulating exosomes and the presence of specific exosome “cargo.” However, their use in diagnostic tests requires an objective and high throughput method of defining their size, concentration, and phenotype in biological fluids. Current methodologies cannot achieve this definition and characterization.

Recognizing this critical issue, during the past 12-month funding period, we demonstrated the feasibility of using nanoparticle tracking analysis (NTA). Although NTA is relatively new and still developing, this technology is well established in other fields, particularly for the measurement of engineered nanoparticles, carbon nanotubes, inks and pigments, and viral particles. The ultimate application of exosome-based diagnostic markers is the ability to identify the presence of circulating cell-derived vesicles and their concentration and size distribution in clinical specimens. We determined the presence and distribution of circulating vesicles in unfractionated sera from ovarian cancer patients, patients with benign disease and female controls (Figure 1). Using the NanoSight LM10, ovarian cancer patients were shown to exhibit ~4-fold increase in the level of total circulating vesicles. The size distribution of these unfractionated vesicles from cancer patients ranged from approximately 50 to 300nm in diameter. Patients with benign disease and controls exhibited a similar size range; however, they possessed a greater percentage of vesicles within the 200-300nm range (versus cancer).

We demonstrated that fractionation of bio-fluids on Sepharose 2B results in two primary peaks of material (Figure 2A): a void volume and a retained peak. We analyzed the individual fractions of the void volume (fractions 15, 16, and 17) using the Nanosight LM10 and NTA software (Figure 2B). NTA demonstrated a very narrow size range of vesicles, with fraction 15 contained vesicles ranging from 50-200nm with a primary peak at 94nm (mode = 94nm, mean = 108, SD = 30nm). Fraction 16 exhibited vesicles also ranging from 50-200nm, but the primary peak appeared at 89nm (mode = 89nm, mean = 95nm, SD = 32nm). Fraction 17 consisted on vesicles ranging from 50-200nm with two principal vesicle peaks at 84nm and 108nm (mode =84, mean = 109, SD =30). Our results demonstrated that the majority of the vesicles within the void volume fractions fall within the 50-100 size range described for exosomes. To define the identity of these vesicles, the current “gold standard” is Western immunoblotting for specific marker proteins. Western immunoblotting of the individual fractions for specific markers claimed to be associated with either exosomes (tetraspanin CD63) or microvesicles (CD154, as known as CD40 ligand). Western immunoblot analysis demonstrated the combined expressions of CD63 and CD154 within the void volume fractions that demonstrate an exosome size distribution. The mutant EGFRvIII, generally considered to be associated with the plasma membrane of cancer cells also appears to be associated with these void volume vesicles, demonstrating the tumor origin of this material. While these vesicles are within the size range of exosomes, they exhibit markers previously defined both as markers for exosomes and microvesicles. Thus, this distinction may not be relevant for clinical specimens.

The “gold standard” for defining the size and characteristics of exosomes is electron microscopy to demonstrate the presence of cup-shaped vesicles, ranging from 50-100nm. This size range was initially defined using exosomes derived from normal lymphocytes. One issue is that size can be modified by sample preparation for EM and the size distribution can be skewed by the image area selected for evaluation (subjective). Since EM studies use pelleted vesicles, image fields where individual vesicles can be visualized may be a limiting factor in this selection. In general, light scattering methodologies report a larger size range than EM and evaluate objectively the total vesicle populations. This study compared these methodologies using chromatographically isolation vesicles. NTA, SPA and DLS were compared with electron microscopic analysis of vesicles: For electron microscopy, the size distribution of vesicles was determined by measuring their diameters directly from electron micrographs of ultracentrifuge pellets. NTA gave a vesicle size distribution from 50 to 175 nm with a mean = 100nm, mode = 87 and SD



= 28. Analysis of the same vesicle preparation by DLS indicated a mean diameter of  $125.3 \pm 1.9\text{nm}$ , while the submicron particle analysis indicated a range of 80 to 120nm. Although the area of the electron microscopy image selected contains vesicles between 50-100nm, While in general EM has been shown to lead to undersizing, vesicles larger than 100nm are clearly visible in multiple fields and the real size distribution of the entire vesicle population is not assessable and EM is not quantitative. DLS and SPA, while providing an objective size distribution of the entire vesicle population, do not define the concentration of the vesicles.

A significant limitation of DLS and SPA is that while they can objectively define the vesicle size range, they cannot define the “phenotype” of these vesicles. Using the NanoSight LM10 equipped with the 405-nm blue-violet laser and more sensitive camera to detect fluorescent particles, quantum dots labeled antibodies reactive with either CD63 (exosomes marker) or EpCAM (marker of vesicles derived from epithelial tumors) labeled vesicles with peaks in the region of 100 nm and 180 nm whether measured in light scatter or fluorescence mode. Vesicles both larger and smaller than 100nm exhibit CD63 demonstrating that the published definition of exosomes as ranging only from 50-100nm may not be accurate.

A criticism of light scattering, Brownian motion based technologies is that these methods do not adequately differentiate between synthetic nanoparticles, large protein aggregates and biologic vesicles. In our size exclusion approach, the void volume fractions contain materials greater than 50 million Daltons, which would be expected to distinguish vesicles from large protein aggregates, including large immune complexes. However, in order to validate that we are differentiating vesicles from large protein complexes, the chromatographically isolated vesicles were initially analyzed by SPA and NTA, followed by a re-analysis after a 5 minute treatment with a non-ionic detergent. Using SPA on the Coulter Model N4 Plus particle size analyzer, the values for vesicle size was observed to range from 80-100nm. Following treatment with 1% Tween 20 for 5 minutes at room temperature, the reanalysis shown that the average size of the particles shifted ~10nm (range 5-20 nm). Using a similar approach with NTA, the same sample treated with 0.5% Triton X100 for 5 minutes at room temperature exhibited a 10-fold reduction.

Vesicle analyses based on light scattering and Brownian motion analyses allow quantitation of mean vesicle size and size distribution. NTA has the additional advantage of defining concentration. The disadvantage of SPA and DLS is that they are unable to determine the phenotype of the vesicles. Since biological fluids and clinical specimens comprise mixtures of vesicles derived from many different cell types, it is essential to be able to determine the cell of origin and to understand their biological function, the molecules that they express on their surface.

An addition critical issue is the separation of tumor-derived exosomes from exosomes released by normal cells presence within the peripheral circulation. To define diagnostic tumor markers, it is essential to identify those actually derived from the tumor. While cell-derived vesicles can be released from many cell types, their accumulation within the peripheral circulation appears to be elevated 3-4-fold in cancer patients. However, since only a fraction of these are produced by the tumor, differentiating the tumor-derived from normal cell-derived exosomes has been problematic. The “background of normal cell-derived exosomes results in significant “noise” in studies failing to separate the tumor-derived exosomes. We have now isolated exosomes from the peripheral circulation of patients with ovarian cancer or from non-tumor-bearing controls by size exclusion chromatography. Further isolation of tumor-specific exosomes by our proprietary method revealed a subpopulation of vesicles within the peripheral circulation with the mean diameter at 72nm. The number of vesicular particles was also determined by the Nanosight analysis, demonstrating the presence of  $2.46 \times 10^{10}$  vesicles/ml (Figure 8). As a proof of concept that the tumor-derived exosome fraction was being isolated, we demonstrated the enrichment of a tumor-specific population was confirmed by the enhanced expression of the tumor marker, EGFRvIII (Figure 9). Thus, analyses of the “cargo” of this enriched tumor derived exosome fraction will allow us to specifically define markers of tumor status and not markers of the patient’s normal cell response to the

tumor. This is critical as the host response is likely to be non-specific (such as a pro-inflammatory immune response) and could result in significant false positive results.

A third critical finding is the selectivity of the exosomal “cargo.” To date, analyses of exosomes and their components have been based on markers demonstrated within the tumor cell and in particular elements apparently up-regulated in the original tumor cells. It has been postulated that components within exosomes are a direct extension of the originating cell. However, our data demonstrate that the miRNAs appearing within the exosomes are highly selective (Figure 10). Of 10 miRNAs on the Cancer miRNA qRT-PCR array previously demonstrated to be elevated in ovarian tumor cells, 8 exhibited significant elevations (greater than 2-fold). 7 miRNAs have been reported to be down-regulated in ovarian tumor cells. Of these, 7 miRNAs only 1 expressed a down-regulation of more than 2-fold (miR-203). Six of these miRNAs were up-regulated by more than 2-fold within exosomes. These results suggest that certain specific miRNAs are “packaged” within exosomes, with little of these miRNAs remaining within the originating cells. In contrast, miRNAs up-regulated within the tumor cells appear to be mirrored by their expression within the exosomes. Thus, we now recognize that some crucial exosomal miRNA markers may not be detectable within the tumor cells.

A fourth finding of the past 12-month funding period was the discovery of long-non-coding RNA. In addition to proteins, lipids and miRNAs, our current work has demonstrated the presence of long noncoding RNAs within exosomes. LncRNAs contribute to genetic regulatory roles, including imprinting, epigenetic regulation, cell cycle control, nuclear and cytoplasmic trafficking, transcription, splicing, cell differentiation and apoptosis. In cancer, the misexpression of lncRNAs contributes to cancer development and progression. Cancer patients exhibit a significant increased level of circulating vesicles in the range of 50-200nm, which exhibited markers confirming their exosome origin. These exosomes contain lncRNA and their profiles were distinct from non-cancer controls. Some lncRNAs, such as MALAT-1 (metastasis-associated in lung adenocarcinoma transcript) were identified in ovarian cancer and demonstrated to be critical in early stage development. Here we demonstrate the elevation of this lncRNA in exosomes from ovarian cancer patients (Figure 14). The stability of exosomes in the peripheral circulation and the unique profile of lncRNAs suggest their ideal utility as a diagnostic biomarker.



## REFERENCES

1. Jemal A, Murray T, Ward E, Samuels A, Tiwari RC, Ghafoor A, Feuer EJ, Thun MJ. Cancer statistics, 2005. *CA: A cancer J for Clinicians*, 55:10-30, 2005.
2. Division of Cancer Prevention and Control, National Center for Chronic Disease Prevention and Health Promotion, 2006.
3. Berek JS, Schultes BC, Nicodemus CF. Biologic and immunologic therapies for ovarian cancer. *J Clin Oncol* 2003; 21(suppl 10): 168-174.
4. Memarzadeh S, Berek JS: Advances in the management of epithelial ovarian cancer. *J Reprod Medicine* 46:621-629, 2001.
5. Hoskins WJ: Prospective on ovarian cancer: Why prevent? *J Cell Biochem* 23 (suppl):189-199, 1995
6. Taylor DD and Gercel-Taylor C: Tumor reactive immunoglobulins. *Oncology Reports*, 1998.
7. Bast RC Jr, Klug TL, St John E. A radioimmunoassay using a monoclonal antibody to monitor the course of epithelial ovarian cancer. *New Engl J Med*, 309:883-887, 1983.
8. Juretzka MM, Barakat RR, Chi DS, Iasonos A, Dupont J, Abu-Rustum NR, Poynor EA, Aghajanian C, Spriggs D, Hensley ML, Sabbatini P. CA125 as a predictor of progression-free survival and overall survival in ovarian cancer patients with surgically defined disease status prior to the initiation of intraperitoneal consolidation therapy. *Gynecol Oncol*, 104:176-180, 2007.
9. Menon U, Jacobs IJ. Recent developments in ovarian cancer screening. *Curr Opin Obstet Gynecol*, 12:39-42, 2000.
10. Petricoin EF, Ardekani AM, Hitt BA, Levine PJ, Fusaro VA, Steinberg SM. Use of proteomic patterns in serum to identify ovarian cancer. *Lancet*, 359:572-577, 2002.
11. Zhang H, Kong B, Qu X, Jia L, Deng B, Yang Q. Biomarker discovery for ovarian cancer using SELDI-TOF-MS. *Gynecol Oncol*, 102:61-66, 2006.
12. Jacobs IJ, Menon U. Progress and challenges in screening for early detection of ovarian cancer. *Mol Cell Proteomics*, 3:355-366, 2004.
13. Taylor DD, Homesley HD, Doellgast GJ (1980) Binding of specific peroxidase-labeled antibody to placental-type alkaline phosphatase on tumour-derived membrane fragments. *Cancer Res* 40: 4064-4069
14. Théry C, Regnault A, Garin J, Wolfers J, Zitvogel L, Ricciardi-Castagnoli P, Raposo G, Amigorena S (1999) Molecular characterization of dendritic cell-derived exosomes. Selective accumulation of the heat shock protein hsc73. *J Cell Biol* 147: 599-610
15. Théry C, Zitvogel L, Amigorena S (2002) Exosomes: composition, biogenesis, and function. *Nat Rev Immunol* 2: 569-579.
16. Taylor DD, Lyons KS, Gercel-Taylor C (2002) Shed membrane fragment associated markers for endometrial and ovarian cancers. *Gynecol Oncol* 84: 443-448
17. Monleon I, M. J. Martinez-Lorenzo, L. Monteagudo, P. Laserra, M. Taules, M. Iturralde, A. Pineiro, M. A. Alava, J. Naval, and A. Anel. 2001. Differential secretion of Fas ligand or APO2 ligand/TNF-related apoptosis-inducing ligand-carrying microvesicles during activation-induced death of human T cells. *J. Immunol.* 167:6736-6744.
18. Raposo, G., D. Tenza, S. Mecheri, R. Peronet, C. Bonnerot, and C. Desaymard. 1997. Accumulation of major histocompatibility complex class II molecules in mast cell secretory granules and their release upon degranulation. *Mol. Biol. Cell.* 8: 2631-2645.
19. Heijnen, H. F. G., A. E. Schiel, R. Fijnheer, H. J. Geuze, and J. J. Sixma. 1999. Activated platelets release two types of membrane vesicles: Microvesicles by surface shedding and exosomes derived from exocytosis of multivesicular bodies and alpha granules. *Blood* 94, 3791-3799.
20. Taylor DD, Black PH (1986) Shedding of plasma membrane fragments: Neoplastic and developmental importance. In: *Developmental Biology* (vol. 3), Steinberg MS (ed) pp 33-57. Plenum Press: New York.
21. Taylor DD, Black PH (1987) Neoplastic and developmental importance of plasma membrane vesicles. *Amer Zool* 26: 411-415

22. Taylor, D.D., Gerçel-Taylor, C., and Weese, J.L. Expression and shedding of mdrl-1 antigen by variants of the murine B16 melanoma. *Surgical Forum*, 40:406-408, 1989.
23. Bazzett, L.B., Magnus, M., Taylor, D.D., Gercel-Taylor, C. Urinary matrix metalloproteinases as a potential screening test for gynecologic malignancies. *Gynecologic Oncology*, 90:435-442, 2003.
24. Taylor, D.D., Gerçel-Taylor, C., and Gall, S.A. Expression and shedding of CD44 isoforms by gynecologic cancer patients. *Journal of the Society for Gynecologic Investigations*, 3:289-294, 1996.
25. Taylor, D.D., Lyons, K.S., and Gercel-Taylor, C. Shed membrane fragment-associated markers for endometrial and ovarian cancers. *Gynecologic Oncology*, 84:443-448, 2002.
26. Mor G, Gutierrez LS, Eliza M, Kahyaoglu F, Arici A. Fas-Fas ligand system-induced apoptosis in human placenta and gestational trophoblastic disease. *Am J Reprod Immunol*, 40:89-94, 1998.
27. Taylor DD, Sullivan SA, Eblen AC, Gercel-Taylor C. Modulation of T-cell CD3-zeta chain expression during normal pregnancy. *J Reprod Immunol*, 54:15-31, 2002.
28. Taylor DD, Gercel-Taylor C. Tumor-derived exosomes as mediators of T-cell signaling defects. *Brit J Cancer*, 92: 305-311, 2005
29. Gorak-Stolinska P, Truman JP, Kemeny DM, Noble A. Activation-induced cell death of human T-cell subsets is mediated by Fas and granzyme B but is independent of TNF-alpha. *J Leuk Biol* 70: 756-766, 2001.
30. Gercel-Taylor C, O'Connor SM, Lam GK, Taylor DD. Shed membrane fragment modulation of CD3-zeta during pregnancy: Link with induction of apoptosis. *J Reprod Immunol*, 56:29-44, 2002.
31. Lagos-Quintana, M., Rauhut, R., Lendeckel, W. & Tuschl, T. Identification of novel genes coding for small expressed RNA. *Science* 294:853-858, 2001.
32. Lau, N. C., Lim, L. P., Weinstein, E. G. & Bartel, D. P. An abundant class of tiny RNAs with probable regulatory roles in *Caenorhabditis elegans*. *Science* 294:858-862, 2001.
33. Lee R C, Ambros V. An extensive class of small RNAs in *Caenorhabditis elegans*. *Science* 294, 862-864, 2001.
34. Ambros V. The functions of animal microRNAs. *Nature* 431:350-355, 2004.
35. Lee Y, Ahn C, Han J, Choi H, Kim J, Yim J, Lee J, Provost P, Radmark O, Kim S, Kim VN. The nuclear RNase Drosha initiates microRNA processing. *Nature* 425:415-419, 2003.
36. Garzon R, Fabbri M, Cimmino A, Calin GA, Croce CM. MicroRNA expression and function in cancer. *Trends in Mol Med*, 12:580-587, 2006.
37. Hammond, S. M. MicroRNAs as oncogenes. *Curr. Opin. Genet. Dev.* 16, 4-9 (2006).
38. Croce CM, Calin GA. (2005). miRNAs, cancer, and stem cell division. *Cell* 122: 6-7.
39. Barad O, Meiri E, Avniel A, Aharonov R, Barzilai A, Bentwich I *et al.* (2004). MicroRNA expression detected by oligonucleotide microarrays: system establishment and expression profiling in human tissues. *Genome Res* 14: 2486-2494.
40. Cummins JM, Velculescu VE. Implications of micro-RNA profiling for cancer diagnosis. *Oncogene*, 25:6220-7, 2006.
41. Calin, G. A. *et al.* Frequent deletions and down-regulation of micro- RNA genes miR15 and miR16 at 13q14 in chronic lymphocytic leukemia. *Proc. Natl Acad. Sci. USA* 99, 15524-15529 (2002). Calin, G. A. *et al.* MicroRNA profiling reveals distinct signatures in B cell chronic lymphocytic leukemias. *Proc. Natl Acad. Sci. USA* 101, 11755-11760 (2004).
42. Iorio, M. V. *et al.* microRNA gene expression deregulation in human breast cancer. *Cancer Res.* 65, 7065-7070 (2005).
43. Ciafre, S. A. *et al.* Extensive modulation of a set of microRNAs in primary glioblastoma. *Biochem. Biophys. Res. Commun.* 334, 1351-1358 (2005).
44. Murakami, Y. *et al.* Comprehensive analysis of microRNA expression patterns in hepatocellular carcinoma and non-tumorous tissues. *Oncogene* 25, 2537-2545 (2006).
45. He, H. *et al.* The role of microRNA genes in papillary thyroid carcinoma. *Proc. Natl Acad. Sci. USA* 102, 19075-19080 (2005).
46. Yanaihara, N. *et al.* microRNA signature in lung cancer diagnosis and prognosis. *Cancer Cell* 9, 189-198 (2006).

47. Cummins, J. M. *et al.* The colorectal microRNAome. *Proc. Natl Acad. Sci. USA* 103, 3687–3692 (2006).
48. Roldo C, Missiaglia E, Hagan JP, Falconi M, Capelli P, Bersani S, Calin GA, Volinia S, Liu CG, Scarpa A, Croce CM. MicroRNA expression abnormalities in pancreatic endocrine and acinar tumors are associated with distinctive pathological features and clinical behavior. *J. Clin. Oncol*, 24:4677–4684, 2006
49. Volinia S, Calin GA, Liu CG, Ambs S, Cimmino A, Petrocca F, *et al.* A microRNA expression signature of human solid tumors define cancer gene targets. *Proc. Natl Acad. Sci. USA* 103:2257–2261, 2006.
50. Esquela-Kerscher A, Slack FJ. Oncomirs- microRNAs with a role in cancer. *Nature Rev. Cancer* 6: 259–269, 2006.
51. Bernstein E, Kim SY, Carmell MA, Murchison EP, Alcorn H, Li MZ *et al.* Dicer is essential for mouse development. *Nat Genet* 35:215–217, 2003.
52. Ali, I. U., Schriml, L. M. & Dean, M. Mutational spectra of PTEN/MMAC1 gene: a tumor suppressor with lipid phosphatase activity. *J. Natl Cancer Inst.* 91:1922–1932, 1999.
53. Iorio, M.V., *et al.* MicroRNA signatures in human ovarian cancer. *Cancer Res.* 67, 8699-8707, 2007.
54. De Cecco, L., *et al.* Gene expression profiling of advanced ovarian cancer: Characterization of a molecular signature involving fibroblast growth factor 2. *Oncogene* 23, 8171-8183, 2004.
55. Calin, G.A. & Croce, C.M. MicroRNA signatures in human cancers. *Nature Rev Cancer* 6, 857-866, 2006.
56. Lu, J. *et al.* MicroRNA expression profiles classify human cancers. *Nature* 435, 834-838, 2005.
57. Storey and Tibshirani, 2003 J.D. Storey and R. Tibshirani, Statistical significance for genomewide studies, *Proc. Natl. Acad. Sci. USA* 100: 9440–9445, 2003.